EPJ Web of Conferences **146**, 05012 (2017) DOI: 10.1051/epjconf/201714605012
ND2016

Resonances in odd-odd ^{182}Ta

C.P. Brits[1,2], M. Wiedeking[2], F.L. Bello Garrote[3], D.L. Bleuel[4], F. Giacoppo[5,6], A. Görgen[3], M. Guttormsen[3], K. Hadynska-Klek[3], T.W. Hagen[3], V.W. Ingeberg[3], B.V. Kheswa[2,3], M. Klintefjord[3], A.C. Larsen[3], K.L. Malatji[2,7], H.T. Nyhus[3], P. Papka[1,2], T. Renstrøm[3], S. Rose[3], E. Sahin[3], S. Siem[3], G.M. Tveten[3], and F. Zeiser[3]

[1] Physics Department, Stellenbosch University, Merriman avenue, Stellenbosch 7600, South Africa
[2] Department of Nuclear Physics, iThemba LABS, PO Box 722, Somerset West 7129, South Africa
[3] Department of Physics, University of Oslo, 0316, Oslo, Norway
[4] Lawrence Livermore National Laboratory, 7000 East Avenue, Livermore 94551, California, USA
[5] Helmholtz Institute Mainz, 55099 Mainz, Germany
[6] GSI Helmholtzzentrum für Schwerionenforschung, 64291 Darmstadt, Germany
[7] Physics Department, University of Western Cape, Modderdam Road, PO Box X17, Bellville 7530, South Africa

Abstract. Enhanced γ-decay on the tail of the giant electric dipole resonance, such as the scissors or pygmy resonances, can have significant impact on (n,γ) reaction rates. These rates are important input for modeling processes that take place in astrophysical environments and nuclear reactors. Recent results from the University of Oslo indicate the existence of a significant enhancement in the photon strength function for nuclei in the actinide region due to the scissors resonance. Further, the M1 strength distribution of the scissors resonances in rare earth nuclei has been studied extensively over the years. To investigate the evolution and persistence of the scissor resonance in other mass regions, an experiment was performed utilizing the NaI(Tl) γ-ray detector array (CACTUS) and silicon particle telescopes (SiRi) at the University of Oslo Cyclotron laboratory. Particle-γ coincidences from the ^{181}Ta(d,p)^{182}Ta and ^{181}Ta(d,d')^{181}Ta reactions were used to measure the nuclear level density and photon strength function of the well-deformed ^{181}Ta and ^{182}Ta systems, to investigate the existence of resonances below the neutron separation energy.

1. Introduction

The photon strength function (PSF) characterises the average electromagnetic properties of an excited nucleus and it is related to radiative decay and photo-absorption processes. The total PSF can be described by various resonances, such as the giant electric dipole resonance (GEDR). The nuclear level density (NLD) is a measurement of the number of levels at a given excitation energy. The PSF and NLD are average properties used to describe the nucleur level structure when it is in the region of the quasi-continuum where the level spacings are comparable to the level widths.

The PSF and NLD are used as input parameters in reaction cross section calculations in the statistical framework of Hauser and Feshback through code like Talys [1], and are relevant to the design of existing and future nuclear power reactors, where simulations depend on the many evaluated nuclear reactions involved [2]. They also play a central role in elemental formation during stellar nucleosynthesis [3]. Calculations have shown that relative small changes to the overall shape of the PSF, can have an order of magnitude effect on the rate of elemental formation [3].

The SR was first observed in well deformed nuclei [4], but it has since been observed in vibrational, transitional and γ-soft nuclei too. The SR has been investigated through nuclear resonance fluorescence (NRF) experiments in various isotopes [5] and also through the Oslo method [6,7] in the rare-earth and actinide regions. Although much knowledge has been obtained about the SR over the years [8], its evolution across the nuclear chart is not well understood. To fully understand the interplay of the SR with other nuclear structures properties, such as coupling to unpaired nucleons and dependence on nuclear shape, the extent and persistence of the SR in transitional regions of the nuclear chart has to be investigated.

2. Experimental setup

The experiment was performed at the cyclotron laboratory of the University of Oslo (OCL) on a self-supporting 0.8 mg/cm^2 thick tantalum target. A 12.5 MeV deuteron beam was used for the reactions ^{181}Ta(d,p)^{182}Ta and ^{181}Ta(d,d')^{181}Ta. The SiRi particle telescope and CACTUS scintillator arrays where used to detect charged particles and γ-rays which were in coincidence with a 2 μs window [9,10].

The SiRi particle telescopes consists of 8 thin, segmented Si ΔE detectors 130 μm thick and 8 E Si detectors 1550 μm thick. These detectors covered scattering angles of $\theta_{lab} = 126^\circ - 140^\circ$ with respect to the beam axis. The CACTUS array consists of 26 NaI(Tl) detectors with $5'' \times 5''$ crystals positioned 22 cm away from the target covering a solid angle of 17% of 4π sr. CACTUS has a total efficiency of 14.1% and an energy resolution of 7% FWHM for a 1332 keV transition.

Table 1. The PSF and NLD normalisation parameters.

Nucleus	D_0 (eV)	$< \Gamma_\gamma(S_n) >$ (meV)	σ (mb)	$\rho(S_n)$ (10^6 MeV^{-1})
^{181}Ta	1.1 ± 0.1	51 ± 1.6	4.9 ± 0.5	2.0 ± 0.30
^{182}Ta	4.2 ± 0.2	59 ± 1.8	5.0 ± 0.5	15.0 ± 3.5

3. Oslo method

By using various analytical techniques the PSF and NLD can be simultaneously extracted using the Oslo method. This method has been covered extensively in the literature [11,12] and only a brief overview will be given here. The first step is to unfold the γ-ray spectra using the detector response function. The Compton background, effects from pair production and the single and double escape peaks are calculated and removed from the γ spectrum. This leaves only full energy deposit events. From the unfolded data the first generation γ-rays can then be extracted. From the distribution of the first generation γ-rays the PSF and NLD can be extracted and normalised.

The decay of a γ-ray to a specific final energy is independent of the reaction that formed the nucleus. This assumption is true for high level densities where the nucleus is in a compound state prior to γ-emission [13]. The probability for a γ-ray to decay from excitation energy E_x to E_f, with energy $E_f = E_x - E_\gamma$, is proportional to the level density at the final energy E_f and the transmission coefficient $T(E_\gamma)$. It is assumed that the transmission coefficient is independent of the initial excitation energy of the nucleus. The first generation γ-ray matrix is proportional to the decay probability and therefore it can be factorised as [11,12]:

$$P(E, E_\gamma) \propto \mathcal{T}(E_\gamma)\rho(E_f) \tag{1}$$

where $\rho(E_f)$ is the level density at the final energy. A χ^2 minimisation between the theoretical and experimental first generation matrix can be used to extract $T(E_\gamma)$ and $\rho(E_f)$. There is an infinite amount of solutions for $P(E, E_\gamma)$ of the form:

$$\tilde{\rho}(E_f) = Aexp[\alpha(E - E_\gamma)]\rho(E_f) \tag{2}$$

$$\tilde{\mathcal{T}}(E_\gamma) = Bexp(\alpha E_\gamma)\mathcal{T}(E_\gamma). \tag{3}$$

Normalization is performed to determine the correct A, B and α values. The NLD is normalised at low energies to experimentally measured levels by simply counting the levels. At the neutron separation energy S_n, normalization is achieved from level densities calculated from neutron resonance spacing data. Since the NLD does not reach S_n the constant temperature model [14] is used to interpolate between the experimental NLD and $\rho(S_n)$. The PSF is normalised from the experimental average total radiative width and given by:

$$f(E_\gamma) = \frac{\tilde{\mathcal{T}}(E_\gamma)}{2\pi E_\gamma^3}. \tag{4}$$

4. Scissors resonance

The SR is a collective excitation mode dominated by single particle events usually found at $E_x = 66\delta A^{1/3}$, where δ is the deformation parameter and A is the nuclear mass [15]. It is a M1 resonance that has been observed in various well deformed nuclei in the rare-earth and actinide regions [6,16]. On a macroscopic level the SR can be described by the oscillation of the proton and neutron distribution against each other, like the blades of a scissors. On a microscopic level the scissors resonance is made up by transitions between levels $\Omega = \Omega \pm 1$ with the same spherical j component. Ω is the quantum number used to describe the projection of the total angular momentum onto the symmetry axis. The experimental SR strength can be estimated by using [6]:

$$B(M1) = \frac{9\hbar c}{32\pi^2}\left(\frac{\sigma\Gamma}{\omega_{M1}}\right), \tag{5}$$

where σ is the cross section, Γ is the radiative width and ω_{M1} is the energy centroid. A theoretical prediction of the SR strength can also be found by using the sum rule approach [17]:

$$B_{M1} = \omega_{M1}\frac{3}{16\pi}\theta_{IV}(g_p - g_n)^2\mu_N^2, \tag{6}$$

where θ_{IV} is the isovector moment of inertia, which here is the rigid-body moment of inertia, g_p and g_n are the bare gyromagnetic factors for protons and neutrons and μ_N is the nucleon magneton. ^{181}Ta is well deformed with a deformation parameter $\delta \sim 0.265$ and ^{182}Ta with $\delta \sim 0.255$ [18]. From this significant deformation, not considering other factors, a strong SR may be expected. Initially, SR experiments only investigated even-even nuclei, since it was thought that in odd-even nuclei the SR strength would be more fragmented, due to the unpaired particle inducing a large fragmentation in the M1 strength distribution [19]. However, contrary M1 strength distributions were eventually found. Some odd-even nuclei, ^{155}Gd, ^{157}Gd, ^{165}Ho, ^{167}Er and ^{169}Tm are characterised by large fragmented M1 strength distributions which may be attributed to the unpaired nucleon [19]. Other odd-even nuclei, ^{161}Dy, ^{159}Tb and ^{163}Dy, however, show localised M1 strength distributions [19]. The investigation for the SR was extended to less deformed nuclei, for example γ-soft, vibrational and transitional nuclei. The SR was found to be reduced by 25% in γ-soft nuclei compared to other good rotors [20]. Additionally tantalum lies in a transitional region of gradual nuclear shape change, which may influence the SR strength.

5. Results

The parameters used for normalising the PSF and NLD are listed in Table 1. The resonance spacing, D_0, and average radiative width $< \Gamma_\gamma(S_n) >$, are averages from values of [21] and [22] and the spin cutoff parameter, σ, is calculated from [23].

The NLD of ^{181,182}Ta are shown in Fig. 1 and the PSF of ^{181,182}Ta are shown in Fig. 2. In order to take the uncertainties of D_0 and $\langle\Gamma_\gamma(S_n)\rangle$ into account, upper

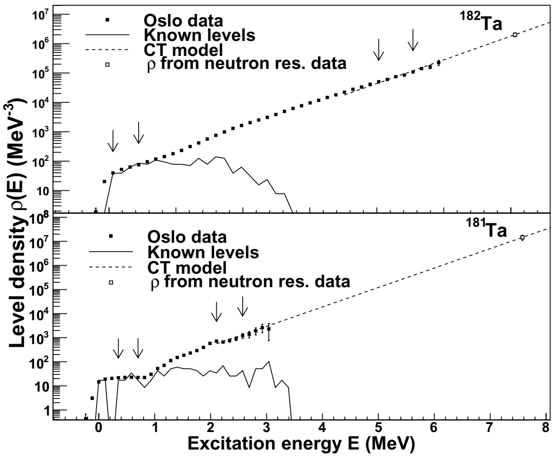

Figure 1. The NLD of ^{181,182}Ta are shown by the filled black squares, the arrows indicate the regions where normalization took place, the open square is the neutron resonance spacing data, the dashed line is the constant temperature model used for extrapolation and the solid line is the known experimental measured level densities [24].

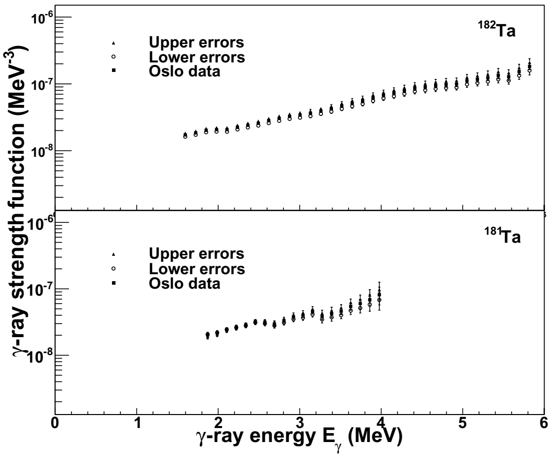

Figure 2. The PSF of ^{181,182}Ta with their respective upper and lower error bands.

and lower limits are defined by $D_0 = D_0 \mp \delta D_0$ and $<\Gamma(S_n)> = <\Gamma(S_n)> \pm <\delta\Gamma(S_n)>$.

The photo absorption cross section data from other measurements can be converted into PSF by [25]:

$$f(E_\gamma) = \frac{\sigma(E_\gamma)}{3E_\gamma(\pi\hbar c)^2}. \quad (7)$$

With the converted PSF data [26–28] the resonances of ^{181,182}Ta are fitted with Lorentzian functions as shown in Fig. 3. The resonances are: an E1 Pygmy resonance (dark blue), a M1 spin-flip resonance (light blue), the split GEDR (purple), the M1 SR (black) and another E1 (green) resonance added so that the total fit matches the experimental data. The GEDR parameters are modified from Ref. [21].

By subtracting the sum of all the resonances, except the SR, arguably only the SR contribution will remain and the strength of the SR can be investigated more accurately. The preliminary SR of ^{181,182}Ta are shown in Fig. 4. The resonances are fit and Eq. (5) is used to calculate

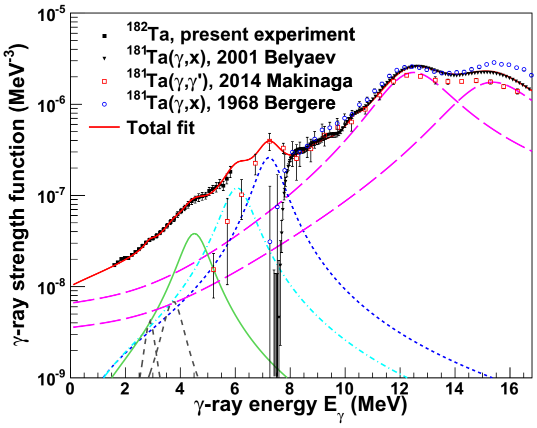

Figure 3. Resonances of ^{182}Ta, see text for details.

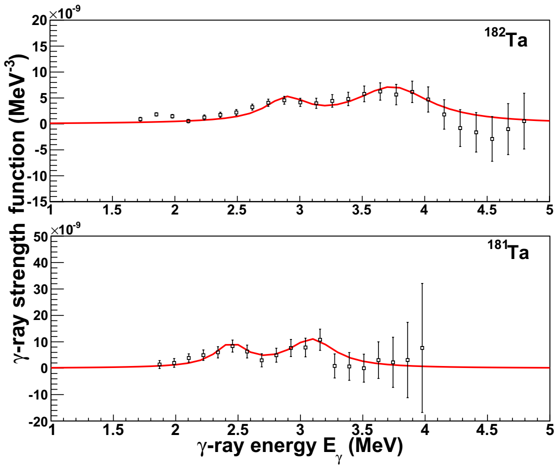

Figure 4. The strength of the SR of ^{181,182}Ta obtained by subtracting the sum of all the other resonances (except the SR) from the total PSF.

the preliminary $B(M_1)$ strengths: $B(M_1) = 3.0^{+0.6}_{-1.0}\,\mu_N^2$ for ^{181}Ta and $B(M_1) = 2.8^{+3.6}_{-2.2}\,\mu_N^2$ for ^{182}Ta. Speculatively we can say the SR strengths are less than the sum rule predictions of (using the experimental energy centroids) 8.9 μ_N^2 and 11 μ_N^2 for ^{181}Ta and ^{182}Ta respectively. This hints at a possible γ-softness. The split SR supports the possible γ-softness, however calculations to refine the results and investigations into this possibility are still ongoing.

6. Conclusion

The PSF and NLD of ^{181}Ta and ^{182}Ta are presented in this paper, from which the SR strength is calculated. In Ref. [29] low-lying excitations of ^{181}Ta were investigated using nuclear resonance fluorescence (NRF) experiments. It was suggested that the scissors resonance was rather weak and split into two parts. The total SR strength in the energy range $E_x = 1.8 - 4$ MeV of ^{181}Ta was found to be $1.3 \pm 0.2\,\mu_N^2$. This is less than 50% compared to ^{181}Ta: $B(M_1) = 3.0^{+0.6}_{-1.0}\,\mu_N^2$ and ^{182}Ta: $B(M_1) = 2.8^{+3.6}_{-2.2}\,\mu_N^2$ from this work.

The SR strength is less than what the sum rule predicts hinting at a possible γ-softness however due to the large uncertainties the SR strengths are uncertain. In order to fully understand the dependence of the SR on unpaired nucleons and nuclear shapes, more data needs to be collected, specifically on nuclei that are γ-soft and odd-odd in nature. Further work is needed to identify the extent and persistence of the SR, in order to understand the evolution of this resonance which can have a significant impact on astrophysical reaction rates.

We would like to thank the operational staff at the OCL for providing excellent experimental conditions. This work was supported by the National Research Foundation of South Africa under grant No. 92789 and the US department of Energy under contract No. DE-AC52-07NA27344. A.C.L. acknowledges support from the ERC-STG-2014 under grant agreement No. 637686 and G.M.T. gratefully acknowledges funding from the Research Council of Norway, project grant No. 222287 and the IAEA under Research Contract 20454.

References

[1] A.J. Koning et al., EDP sciences; eds. O. Bersillon et al. p. 211 (2008), see also `www.talys.eu`
[2] M.B. Chadwick et al., Nucl. Data Sheets **112**, 2887 (2011)
[3] S. Goriely, Phys. Lett. B **436**, 10 (1998)
[4] D. Bohle et al., Phys. Lett. B **137**, 27 (1984)
[5] U. Kneissl, H.H. Pitz, A. Zilges, Prog. Part. Nucl. Phys. **37**, 349 (1996)
[6] M. Guttormsen et al., Phys. Rev. Lett. **109**, 162503 (2012)
[7] T. Laplace et al., Phys. Rev. C **93**, 014323 (2016)
[8] P. von Neumann-Cosel, K. Heyde, A. Richter, Rev. Mod. Phys. **82**, 2365 (2010)
[9] M. Guttormsen et al., Phys. Src. **T32**, 54 (1990)
[10] M. Guttormsen et al., Nucl. Instrum. Methods Phys. Res. Sect. A **648**, 168 (2010)
[11] A. Schiller et al., Nucl. Instrum. Methods Phys. Res. A **447**, 498 (2000)
[12] A.C. Larsen et al., Phys. Rev. C **83**, 034315 (2011)
[13] J. Rekstad et al., Phys. Scr. **T5**, 45 (1983)
[14] A. Gilbert, A.G.W. Cameron, Can. J. of Phys. **43**, 1446 (1965)
[15] A. Richter, Prog. Part. Nucl. Phys. **34**, 261 (1995)
[16] S. Siem et al., Phys. Rev. C **65**, 044318 (2002)
[17] E. Lipparini, S. Stringari, Phys. Rep. **175**, 103 (1989)
[18] S. Hilaire, M. Girod, AIP conference proceedings **1012**, 359 (2008)
[19] J. Ender et al., Phys. Rev. Lett. **79**, 2010 (1997)
[20] P. von Brentano et al., Phys. Rev. Lett. **76**, 2029 (1996)
[21] R. Capote et al., *Reference input parameter library, ripl-2 and ripl-3*, `http://www-nds.iaea.org/RIPL-3/`
[22] S.F. Mughabghab, *Atlas of Neutron Resonance*, 5th edn. (Elsevier Science, Amsterdam, 2006)
[23] T. von Egidy, D. Bucurescu, Phys. Rev. C **80** (2009)
[24] Brookhaven National Laboratory, *A database of nuclear levels*, `http://www.nndc.bnl.gov/chart`, retrieved 2015
[25] F. Giacoppi et al., Phys. Rev. C **91**, 054327 (2015)
[26] A. Makinaga et al., Phys. Rev. C **90**, 044301 (2014)
[27] S.N. Belyaev, V.P. Sinichkin, Workshop on beam dynamics and optimization, Saratov, p. 81 (2001)
[28] H. Beil, R. Bergere, A. Veyssiere, Nucl. Phys. **121**, 463 (1968)
[29] A. Wolpert et al., Phys. Rev. C **58**, 765 (1998)